ROYAL SOCIETY OF CHEMISTRY

EDGE ARTICLE

CrossMark
click for updates

Carbide complexes as π-acceptor ligands†

Anders Reinholdt, Johan E. Vibenholt, Thorbjørn J. Morsing, Magnus Schau-Magnussen, Nini E. A. Reeler and Jesper Bendix*

The π-accepting character of a terminal carbide complex acting as a ligand is demonstrated experimentally and corroborates earlier theoretical predictions. As a result, coordination of a terminal ruthenium carbide complex to electron-rich metal centres is shown to provide a facile and versatile route to carbide-bridged heterometallic complexes. Synthesis, reactivity, spectroscopic and structural characterization are reported for heterobimetallic systems with auxiliary metals from groups 9–11: Rh(I), Ir(I), Pd(II), Pt(II), Ag(I), and Au(I) coordinated by $[Ru(C)Cl_2(PCy_3)_2]$ (**RuC**). This encompasses the first example of a homoleptic carbide-ligated transition metal complex: $[\{(Cy_3P)_2Cl_2RuC\}_2Au]^+$. Kinetics of substitution on Pt(II) by **RuC** ranks the carbide complex as having intermediate nucleophilicity. The ^{13}C-NMR signals from the carbide ligands are significantly more shielded in the bridged heterobimetallic complexes than in the parent terminal carbide complex. Structurally, **RuC** forms very shorts bonds to the heterometals, which supports the notion of the multiple bonded complex acting as a π-backbonding ligand. Reactions are reported where **RuC** displaces CO coordinated to Rh(I) and Ir(I). A strong *trans* influence exerted by **RuC** indicates it to be a stronger σ-donor than CO. The geometries around the carbide bridges resemble those in complexes of electron-rich metals with carbonyl or bridging nitride-complex-derived ligands, which establishes a link to other strong π-acceptor ligands.

1 Introduction

Mono-atomic carbon as a ligand is not common. Nevertheless, it has implications to all forms of life as it was recently shown to be present in nitrogenase,[1–4] which is responsible for the conversion of atmospheric nitrogen into bioavailable ammonium. The most effective nitrogenase has an FeMo cofactor active site containing a six-coordinate interstitial carbon. Mono-atomic carbon ligands are also of relevance in large-scale industrial heterogeneous catalysed processes such as fuel synthesis by the Fischer–Tropsch process[5,6] which encompasses the catalytic hydrogenation and polymerization of CO into alkanes and oxygenated compounds. Here terminal carbon ligands form on the surface of Fischer–Tropsch catalysts and possibly play a role in the formation of C–C bonds in the products.[7]

Terminal carbide complexes are rational precursors for carbide-bridged complexes as the commodious, one-coordinate carbide ligand in an M≡C: unit allows an incoming metal centre to approach and be ligated, but this approach is virtually unexplored. Generally, routes to heterometallic carbide-bridged systems are singular in the sense that they have a limited scope for generalization to other metals. However, one notable example of a versatile route to bimetallic carbide-bridged complexes is Templeton's and Hill's development of the $(Tp^*)(OC)_2MC–M'$ platform (M = Mo, W, M' = Si, Ge, Sn, Pb,[8] Fe,[9] Ni,[10] Au,[11] Hg,[12] Tp^{*-} = hydridotris(3,5-dimethyl-pyrazol-1-yl)borate). Terminal carbides have been isolated for 2nd and 3rd row group 6 (ref. 13 and 14) and group 8 (ref. 15–19) transition metals. The known terminal carbides of molybdenum and tungsten are very sensitive to air and moisture and must be handled under inert atmospheres. Similarly, in bimetallic group 6 complexes, bridging carbide ligands are prone to associate with non-metals affording μ-CR ligands (R = H,[20] R = PEt_3,[10] Et = ethyl).

Contrarily, the terminal ruthenium carbide complex, $[Ru(C)Cl_2(PCy_3)_2]$ (**RuC**), is remarkably stable in air in which it may be handled and stored for years without apparent decomposition. Heppert's serendipitous discovery[15] of the metathesis-facilitated route to **RuC** and Grubbs' rational extension[16] based on phosphine-exchange reactions offered the terminal carbide readily, though with the requirement for rather complex organic reagents. This was circumvented in Johnson's elegant synthesis[17] of **RuC**, which employed commonplace vinyl acetate *in lieu* of Feist's esters. The stability combined with straightforward ^{13}C-labeling of the terminal carbide ligand[17,21] simplifies attempts at a rational bottom-up approach to carbide-bridged systems and led us to investigate the reactivity

Department of Chemistry, University of Copenhagen, Universitetsparken 5, DK-2100, Denmark. E-mail: bendix@kiku.dk; Tel: +45 35320101
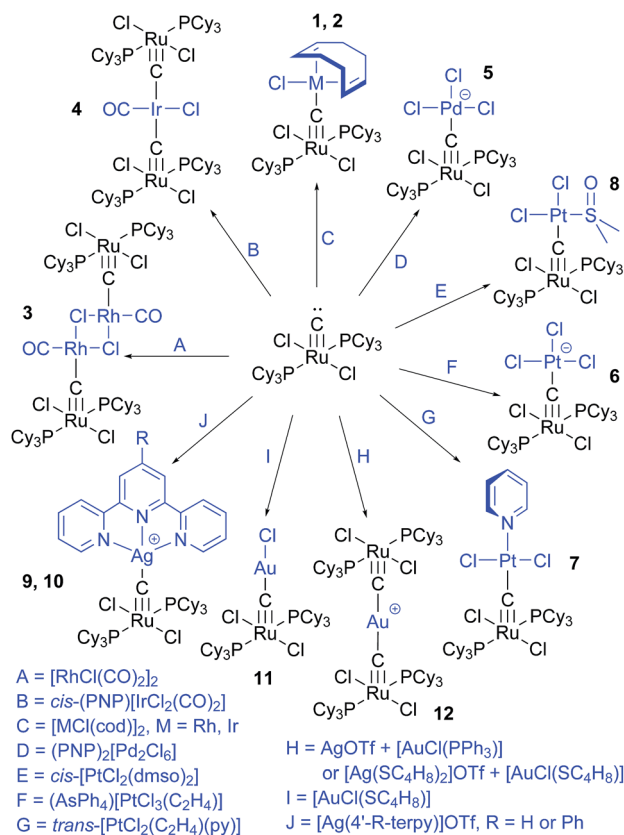
Scheme 1 Synthesis of carbide-bridged complexes.

of **RuC** as a ligand. Among the known reactions of **RuC** are oxidations to yield $[Ru(CO)Cl_2(PCy_3)_2]$, $[Ru(CS)Cl_2(PCy_3)_2]$,[17] and $[Ru(CSe)Cl_2(PCy_3)_2]$.[22] On reaction with strong acids, the protonated carbide associates with a phosphine to yield phosphonium alkylidenes, $[(Cy_3P)Cl_2Ru=CH(PCy_3)]X$,[19,23] $X = BF_4^-$, $B(C_6F_5)_4^-$, OTf^- ($OTf^- =$ trifluoromethanesulfonate). Reactions of **RuC** with $MeO_2CC\equiv CCO_2Me$, MeOTf, and the tropylium ion yield $[(Cy_3P)_2Cl_2Ru=CC_2(CO_2Me)_2]$,[21] $[(Cy_3P)_2Cl_2Ru\equiv CMe]OTf$,[18] and $[(Cy_3P)_2Cl_2Ru\equiv CCH_2C_6H_5]^+$,[18] respectively. These protonations and alkylations demonstrate that **RuC** reacts as a nucleophile, though it appears a rather weak nucleophile, as it fails to react with even fairly reactive electrophiles such as MeI, MeCOCl, and $C_6H_5CH_2Br$.[21] Along these lines, Grubbs and co-workers reported the formation of heterometallic carbide-bridged complexes assembled from **RuC** and Pd(II) or Mo(0) with the argument that the ruthenium carbide functions as a σ-donating ligand towards these metal centres.[16]

In coordination chemistry, molecular complexes with mono-atomic carbon ligands are scarce in comparison with the numerous complexes with mono-atomic N, O, and F ligands. For the latter ligands, their oxidation state is generally not ambiguous, and they can be viewed as isoelectronic N^{3-} (nitride), O^{2-} (oxide) and F^- (fluoride) ligands although some complexes of mono-atomic nitrogen are best considered nitrene (N^-) complexes. Mono-atomic carbon ligands are often referred to as carbide ligands, implying C^{4-}, by analogy with the above isoelectronic series. However, for carbon a quite clear

dichotomy exists between the formulation as carbide or carbon (C^0) ligands. Thus, based on the computational studies of charge density distributions in $Fe(C)(CO)_4$, Frenking suggested a nomenclature for carbon-containing ligands that classifies **RuC** as a carbon complex.[24] We do not dispute this result, but prefer in the following to denote **RuC** and the derived systems as carbide complexes in agreement with common usage and in line with their very strong resemblance in both structure and reactivity to established *bona fide* nitride complexes.

Computational studies of terminal carbide complexes of group **8** metals reveal metal carbide triple bonds that are polarized toward the metal[24] and carbon-based lone pairs with a large degree of 2 s character.[25] This corresponds well with the experimentally observed weak nucleophilic character exhibited by the carbide ligand in **RuC**. In addition to σ-donating properties, the presence of energetically low-lying unoccupied molecular orbitals with local π-symmetry suggests the suitability of the carbide moiety for coordination to electron-rich transition metals as a back-bonding ligand.[26] Frenking compared metal carbon complexes with carbon monoxide in terms of their donor–acceptor interactions as ligands.[27] Based on orbital energies, the metal carbon complexes were argued to be promising, possibly better σ-donating ligands than CO and *comparably good π-accepting* ligands. Thus, it was suggested that metal carbon complexes could potentially outcompete CO as a ligand toward transition metal centres and that the formation of homoleptic carbon-bridged complexes might be achieved, since homoleptic carbonyl complexes are stable and numerous.

The electronic structure of terminal carbide complexes has a counterpart in the coordination chemistry of the isoelectronic terminal nitride complexes. Based on the spatial and orbital relationships between CO and terminal nitride complexes, and corroborated by experimental data, Mayer and co-workers originally proposed that terminal nitrides can function as strong π-accepting ligands.[28] In the following, we demonstrate the same to be the case for terminal carbides and thereby experimentally establish a link between terminal carbides, terminal nitrides, and CO as ligands.

2 Results and discussion

Carbide-bridged systems form smoothly (*vide infra*) when solutions of **RuC** in CH_2Cl_2 or $CHCl_3$ are treated with complexes of electron-rich metals with displaceable ligands (Scheme 1). This furnishes a general route to the heterometallic carbide-bridged complexes $[(Cy_3P)_2Cl_2RuC–RhCl(cod)]$ (**1**), $[(Cy_3P)_2Cl_2RuC–IrCl(cod)]$ (**2**), $[(Cy_3P)_2Cl_2RuC–RhCl(CO)]_2$ (**3**), $[\{(Cy_3P)_2Cl_2RuC\}_2IrCl(CO)]$ (**4**), $(PNP)[(Cy_3P)_2Cl_2RuC–PdCl_3]$ (**5**), $(AsPh_4)[(Cy_3P)_2Cl_2RuC–PtCl_3]$ (**6**), $[(Cy_3P)_2Cl_2RuC–PtCl_2(py)]$ (**7**), $[(Cy_3P)_2Cl_2RuC–PtCl_2(dmso-S)]$ (**8**), $[(Cy_3P)_2Cl_2RuC–Ag(terpy)]OTf$ (**9**), $[(Cy_3P)_2Cl_2RuC–Ag(4'-Ph-terpy)]OTf$ (**10**) $[(Cy_3P)_2Cl_2RuC–AuCl]$ (**11**), and $[\{(Cy_3P)_2Cl_2RuC\}_2Au]OTf$ (**12**).‡ Fig. 1 depicts the molecular structures of complexes **1**–**12**. The conformations near the heterometal carbide bonds demonstrate the requirement for space exerted by the bulky tricyclohexylphosphines in **RuC**. Thus, ligands on the heterometals lie in a plane nearly perpendicular to the phosphine–ruthenium bonds. This is readily apparent from

inspection of the molecular structures of **1–10**, whose hetero-metal centres have square planar ligand arrangements.

The dimeric group **9** metal complexes, $[RhCl(cod)]_2$ and $[IrCl(cod)]_2$, undergo symmetric cleavage of their chloride-bridged cores upon reaction with **RuC** to form $[(Cy_3P)_2Cl_2RuC–RhCl(cod)]$ (**1**) and $[(Cy_3P)_2Cl_2RuC–IrCl(cod)]$ (**2**). On the other hand, $[RhCl(CO)_2]_2$ reacts differently from the cyclooctadiene complexes: the chloride-bridged core in $[RhCl(CO)_2]_2$ persists, and **RuC** displaces one CO ligand from each metal centre to form the tetranuclear structure, $[(Cy_3P)_2Cl_2RuC–RhCl(CO)]_2$ (**3**). The carbides are arranged *trans* with respect to the chloride bridges between the Rh centres. Mononuclear *cis*-(PNP)[IrCl_2-(CO)_2] reacts with **RuC** to lose both a CO and a Cl^- affording the neutral *trans*, bis complex, $[\{(Cy_3P)_2Cl_2RuC\}_2IrCl(CO)]$ (**4**).

The reactivity of divalent group **10** metal centres resembles that of the monovalent group **9** metals. Thus, **RuC** cleaves the dichloride bridge in the anion of dimeric $(PNP)_2[Pd_2Cl_6]$ to form $(PNP)[(Cy_3P)_2Cl_2RuC–PdCl_3]$ (**5**), and the same motif of reactivity is observed in the reaction of **RuC** with the anion of Zeise's salt, $[PtCl_3(C_2H_4)]^-$, to yield $(AsPh_4)[(Cy_3P)_2Cl_2RuC–PtCl_3]$ (**6**), whose anion is isostructural to the anion of **5**. Reactions of **RuC** with *trans*-[PtCl_2(C_2H_4)(py)], and *cis*-[PtCl_2(dmso-S)_2] result in displacement of ethene or dmso to yield *trans*-$[(Cy_3P)_2Cl_2RuC–PtCl_2(py)]$ (**7**) and *cis*-$[(Cy_3P)_2Cl_2RuC–PtCl_2(dmso-S)]$ (**8**), respectively. This shows that **RuC** is a good ligand towards Pt(II) as it outcompetes the soft ligands, C_2H_4 and dmso. An alternative route to **7** starts from **6**, which reacts with pyridine to substitute the chloride *trans* to the carbide bridge. The kinetics

of ligand substitution in *cis*-[PtCl_2(dmso-S)_2] to yield **8** was investigated (*cf.* ESI incl. Fig. S16†) and the reaction was found to occur with a second-order rate constant of $k_2 = 0.27(3)$ M^{-1} s^{-1}, which is an intermediate rate for substitution in this class of systems ranking **RuC** comparable to thiocyanate and sulphite in terms of nucleophilicity.[29,30]

Among the simplest conceivable routes to carbide-bridged complexes of group **11** metals are reactions between **RuC** and simple silver salts such as AgOTf, but these reactions failed to give isolable products. On the other hand, triflate salts of the silver complexes, $[Ag(terpy)]^+$ and $[Ag(4'-Ph-terpy)]^+$ react with **RuC** to give $[(Cy_3P)_2Cl_2RuC–Ag(terpy)]OTf$ (**9**) and $[(Cy_3P)_2Cl_2RuC–Ag(4'-Ph-terpy)]OTf$ (**10**). The reactivity of **RuC** towards gold(I) complexes varies in a subtle manner: $[AuCl(SC_4H_8)]$ (SC_4H_8 = tetrahydrothiophene) readily dissociates SC_4H_8 in favour of **RuC** to form $[(Cy_3P)_2Cl_2RuC–AuCl]$ (**11**). On the contrary, no reaction occurs between $[AuCl(PPh_3)]$ and **RuC**. Initial treatment with AgOTf generates AgCl and formal $[Au(PPh_3)]^+$ that reacts with **RuC** to form $[(Cy_3P)_2Cl_2RuC–AuPPh_3]^+$ as characterized by NMR (*vide infra*). The presence of **RuC** renders PPh₃ labile, and another **RuC** associates with the gold centre, yielding the homoleptic carbide-bridged complex, $[\{(Cy_3P)_2Cl_2RuC\}_2Au]OTf$ (**12**). An alternative route to **12** uses $[Ag(SC_4H_8)_2]OTf$ and $[AuCl(SC_4H_8)]$ to generate Au(I) with all labile ligands, which subsequently reacts with two equivalents of **RuC**. The existence of **12** indicates the stability of the gold carbide bond and confirms the predicted feasibility of formation of homoleptic carbide-ligated complexes, though it is
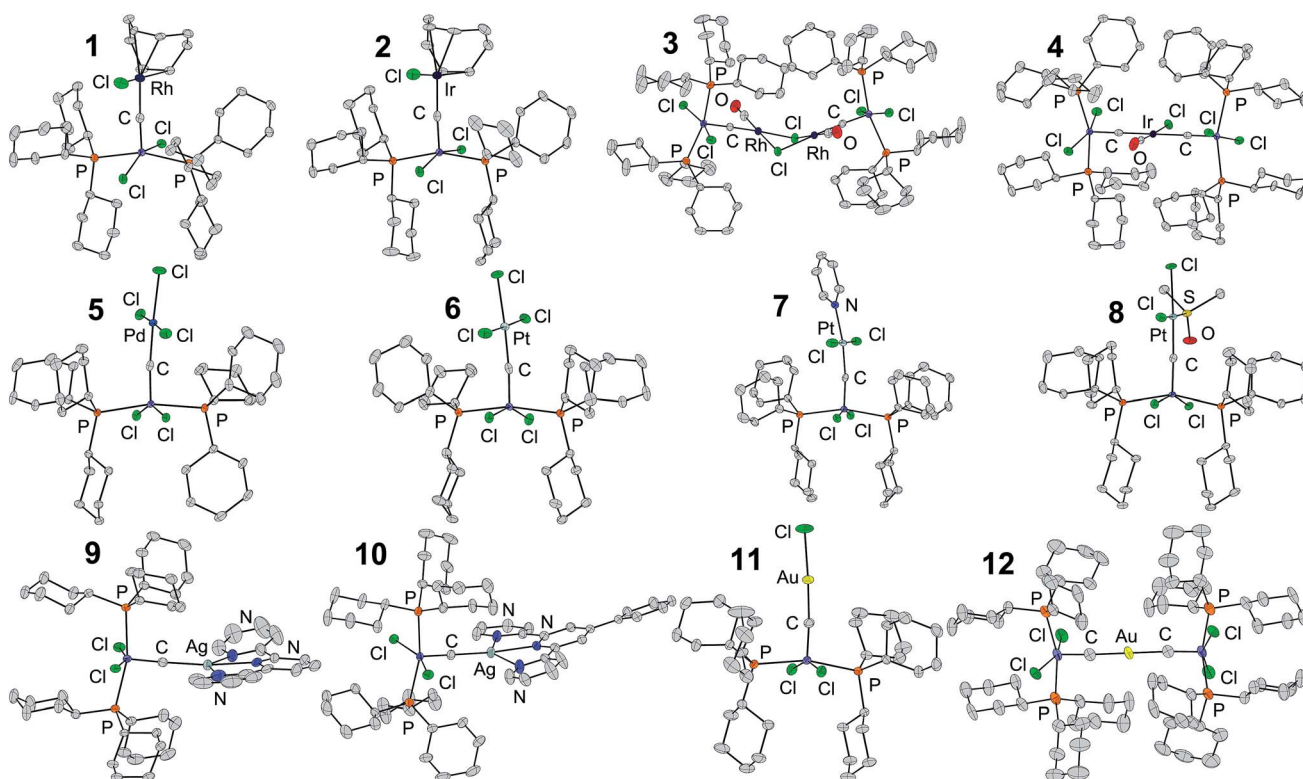

Fig. 1 Molecular structures of the carbide-bridged systems **1–12**. Displacement ellipsoids correspond to 50% probability. H-atoms, co-crystallised solvent molecules and counter ions, PNP^+ (**5**), $AsPh_4^+$ (**6**), OTf^- (**9** and **10**), and BF_4^- (**12**) are omitted.

achieved for much lower coordination numbers than the ones discussed by Frenking.[27] The structural determination of the homoleptic complex suffered from disorder problems with triflate as the counterion, and consequently, the corresponding BF_4^- salt was prepared by the first route using $AgBF_4$.

2.1 Spectroscopic evidence of π-backbonding

Some insight into the bonding situation can be gained from vibrational spectroscopy. Vaska's complex (*trans*-[IrCl(CO)(PPh₃)₂])[31] and **4** belong to the same family of complexes, *trans*-[IrCl(CO)L₂], which allows for a direct comparison of their solid state infrared (IR) carbonyl stretching frequencies. Within Vaska-like complexes, ν_{CO}/cm^{-1} increases in the order: L = PCy₃ (1934)[32] < PPh₃ (1954)[32] < P(CH₂CH₂(CF₂)₅CF₃)₃ (1975)[33] < P(C₆F₅)₃ (1994);[34,35] in **4**, ν_{CO} is 1990 cm⁻¹ (*cf.* ESI Fig. S14†). The phosphines in Vaska-like complexes presumably function as π-accepting ligands,[36,37] and in terms of π-accepting strength, this consequently ranks **RuC** on a par with the strongest π-accepting phosphines.

Raman spectroscopy combined with isotopic labelling identifies the stretching frequencies that relate to the carbide ligands in **RuC** (¹²C, ¹³C: 1050, 1013 cm⁻¹) and **11** (¹²C, ¹³C: 1145, 1103 cm⁻¹) (*cf.* ESI Fig. S11 and S12†). Naively, the shift would suggest a strengthening of the Ru≡C bond upon coordination, which would contrast with **RuC** acting as a π-accepting ligand towards gold(I). However, the literature provides examples of increase in stretching frequencies of metal nitride multiple bonds upon coordination to main group element and transition metal fragments: the IR stretching frequency of the nitride ligand in (NBu₄)[Os(N)O₃] (1023 cm⁻¹) increases on coordination to [AuPPh₃]⁺ (1102 and 1088 cm⁻¹) and *cis*-[Pt(PMe₃)₂]²⁺ (1088 and 1072 cm⁻¹).[38] Similarly, the stretching frequency of nitride in Re(N)Cl₂(PMe₂Ph)₃ (1061 cm⁻¹)[39] increases on coordination to [AuCl] (1125 cm⁻¹)[40] and [BCl₃] (1180 cm⁻¹).[41] These observations have been rationalized[41] as the result of coupled vibrations in the Re≡N–X moieties that shift $\nu_{Re\equiv N}$ and ν_{N-X} to higher and lower wavenumbers, respectively. Based on this, it must be concluded that stretching frequencies of the Ru≡C bonds are unsuited as probes for π-backdonation from the metal fragments coordinated to **RuC**.

The facile labelling of the carbide ligand in **RuC** makes ¹³C-NMR a useful handle on the reactivity and electronic structure of the derived heterometallic systems. Signals from carbide bridges (δ_C = 345–434 ppm) and resonances from organic carbons and unreacted **RuC** (472 ppm) are easily discriminated by ¹³C{¹H}-NMR (*cf.* Table 1). The upfield shift of the carbide resonance upon bridging demonstrates increased shielding, suggesting increased electron density around the carbide. This corresponds well with the notion that **RuC** functions as a π-accepting ligand. However, this view is too simplistic, as the least backbonding heterometal centres, Pt(II) and Pd(II), provide the largest shifts in δ_C. Rather, the internal shielding in the Ru≡C moiety needs to be factored in, as is the case for carbonyl complexes.[42]

Heterometal to carbide NMR coupling constants (Table 1) serve as fingerprints of coordination and handles on

Table 1 ¹³C-NMR chemical shifts (δ_C) and coupling constants (J_{C-M}) from the carbide-bridged complexes, **1–12**. J_{C-M} for **9** and **10** are approximate since couplings to ¹⁰⁷Ag and ¹⁰⁹Ag are close in magnitude

Complex	δ_C (ppm)	J_{C-M} (Hz)
1	411.7	59.1
2	387.6	—
3 (CRu)	396.4	60.2
3 (CO)	177.7	85.6
4	397.4	—
5	380.9	—
6	344.7	1395.5
7	350.3	1283.4
8	349.0	1333.8
9	433.5	187.0
10	433.1	187.8
11	395.3	—
12	395.3	—

backbonding in the carbide-bridged complexes. For instance, the isostructural complexes, **1** and **2**, are readily distinguished by ¹³C-NMR: the carbide bridge in the iridium complex yields a singlet at 387.6 ppm whereas the carbide bridge in the rhodium complex yields a doublet (411.7 ppm, J_{C-Rh} = 59.4 Hz). The carbide bridge in **3** (397.4 ppm) yields a doublet with nearly the same coupling constant as in **1** (59.0 Hz), while the carbonyl ligand in **3** couples more strongly to Rh than the carbide (J_{C-Rh} = 85.6 Hz). This stronger coupling parallels shorter bonds from rhodium to the carbonyl ligands than to the carbide ligands (*vide infra*). As expected, the carbide bridge signals from **6–8** display satellite peaks due to ¹⁹⁵Pt (J_{C-Pt} = 1283.4–1395.5 Hz), and those from **9** and **10** appear as broadened doublets due to coupling to both ¹⁰⁷Ag and ¹⁰⁹Ag (J_{C-Ag} = 187.0–187.8 Hz).

2.2 Reactivity of heterometallic systems

The stepwise formation of the homoleptic gold(I) complex, **12**, through the intermediate, [(Cy₃P)₂Cl₂RuC–AuPPh₃]⁺, is clearly evident from ¹³C-NMR as the reaction mixture yields a doublet in the carbide range δ = 411.0 ppm, J_{C-P} = 108.7 Hz. This coupling is significantly larger than typical coupling constants between the bridging carbide and the PCy₃ ligands (5.6–7.5 Hz). The isolable product of the reaction, **12**, yields a broad singlet (395.3 ppm) without discernible couplings to phosphorus, consistent with the absence of PPh₃ in the final product.

The combination of solid-state structures and ¹³C-NMR data also provides insight into the reactivity of the carbide-bridged systems (*cf.* Scheme 2). Compound **6** loses the chloride ligand on Pt(II) positioned *trans* to the bridging carbide when treated with pyridine. This alternative route to **7** shows that the larger structural *trans* influence of the carbide ligand compared to that of chloride (*vide infra*) is accompanied by a preference for *trans* substitution. Additionally, NMR reveals that **11** is suited as precursor for other systems, as it undergoes transmetallation with appropriate metal complexes. Hence, [RhCl(cod)]₂, [IrCl(cod)]₂, [RhCl(CO)₂]₂, and (AsPh₄)[PtCl₃(C₂H₄)] slowly react

with **11** to form **1**, **2**, **3**, and **6**, respectively. The reaction with [RhCl(CO)₂]₂ first generates an intermediate (393.3 ppm, $J = 60$ Hz) that reacts further to yield **3**.

2.3 Structural influence of the Ru≡C moiety

Table 2 contains metrics for the carbide-bridged systems investigated here. To a first approximation, the geometries around the carbide bridges correspond to sp-hybridized C with a triple bond to Ru and a single bond to the heterometal: the carbide bridges are linear (172.9(2)–180°), and the short Ru–C triple bonds fall in the range 1.642(3)–1.698(3) Å corresponding to modest elongations of 0.6–4.0% of the triple bond in the precursor **RuC**. The assignment with carbide forming a triple and a single bond agrees with the suggestion by Hoffmann and co-workers[43] that in the series M–X–M (M = transition metal, X = F⁻, O²⁻, N³⁻, and C⁴⁻), the tendency is for the X bridge to become increasingly asymmetric as its electronegativity decreases. However, counterexamples for carbide-containing homometallic, symmetric M–C–M bridges, *e.g.* M = Nb,[44] Re,[45] Fe,[46–50] and Ru,[51] exist.

The only previously reported system belonging to the present class, which has been structurally characterized, namely Grubbs' *trans*-[(Cy₃P)₂Cl₂RuC–PdCl₂(SMe₂)],[16] provides a good basis for comparison with **5** as it contains **RuC** linearly coordinated to Pd(II). The Ru–C triple bond is 0.4% shorter than in **5**, and the C–Pd single bond is 2.9% longer than in **5**. The palladium carbide bond in **5** falls within the range of platinum carbide bond lengths spanned by the Pt(II) complexes **6–8**. Compared with its most obvious congener, **6**, the Pd–C bond in **5** is longer than the Pt–C bond by 0.019 Å (1.0%). This similarity between the Pd(II) and Pt(II) systems is mirrored by the Rh(I) and Ir(I) complexes **1** and **2**. Here, bond distances that involve the carbide are identical within 3σ, underlining the geometric similarity between the rhodium and iridium complexes. On the other hand, the iridium carbide bonds in **4** are distinctly longer (0.092–0.106 Å) than those in **2**. This is in part caused by the large structural *trans* influence of **RuC** (compared to Cl⁻, *vide infra*) and in part by the severe steric crowding from two **RuC**,

Table 2 Carbide bridge metrics from X-ray crystallography. Percentile rank compares the metal carbide distance to any M–C bond distance from the CSD

| Complex	Ru–C–M (°)	Ru–C (Å)	C–M (Å)	Percentile rank (%)
1	173.4(1)	1.690(2)	1.897(2)	10.0
2	174.75(15)	1.698(3)	1.882(3)	8.9
3	176.88(13)	1.688(2)	1.864(2)	7.4
4[a]	180	1.677(5)	1.988(5)	16.5
	180	1.675(5)	1.974(5)	15.5
5	173.50(15)	1.668(2)	1.892(2)	0.5
6	174.4(2)	1.691(3)	1.873(3)	4.2
7	172.9(2)	1.679(3)	1.882(3)	4.9
8	177.6(1)	1.682(2)	1.919(2)	6.9
9	177.23(15)	1.642(3)	2.082(3)	17.6
10	176.5(2)	1.651(3)	2.072(3)	13.4
11	175.4(2)	1.664(3)	1.921(3)	2.3
12[a]	173.6(6)	1.679(10)	1.960(10)	9.1
	175.4(6)	1.655(9)	1.974(9)	14.3

[a] **4** and **12** crystallize with two crystallographically independent carbide bridges, with identical connectivity.

Cl⁻, and CO in the ligand sphere of **4**. Similarly, the gold carbide bonds in **12** are longer than those in **11**. The shortening of the RuC–M bonds seen for 5d *vs.* 4d metals becomes more pronounced with increasing group number: in group 11, **9** and **10** have significantly longer Ag–C bonds than the Au–C bonds in **11** and **12**.

Due to its unique nature, straight-forward structural analogues for comparisons with **12** do not exist. However, Hill and co-workers[11] reported the tetrameric homoleptic carbide-bridged gold complex, [(Tp*)(OC)₂W(μ₃-C)Au]₄. As opposed to the exclusive end-on binding mode in **12**, the tetrameric gold complex has the tungsten carbide coordinated to Au(I) with both end-on and side-on binding modes, which enforces significantly bent carbide bridges (160.3(12)–167.7(12)°). The end on Au–C bonds are at 1.971(19)–2.03(2) Å, comparable to or slightly longer than the Au–C bonds in **11** and **12**, and the side on Au–C bonds are longer (2.03(2)–2.14(2) Å).

In **12**, carbide and gold(I) take on inverted roles compared to the homoleptic gold carbides studied by Schmidbaur and co-workers:[52–58] the [(R₃PAu)₆C]²⁺ and [(R₃PAu)₅C]⁺ complexes contain carbide with a coordination sphere composed only of gold(I), whereas the coordination sphere of gold(I) in **12** is composed only of carbide.

On the heterometal centres in **1**, **2**, **5**, and **6**, chloride and the bridging carbide are positioned *trans* to the same ligands, which allows for a direct comparison of their *trans* influences. In **1**, the average Rh–C distance (C belonging to cod) is 2.139 Å *trans* to Cl⁻ and 2.305 Å *trans* to carbide. Equivalently, *trans* to Cl⁻ and carbide the Ir–C distances in **2** are 2.134 Å and 2.291 Å, the Pd–Cl distances in **5** are 2.3079 Å and 2.3276(7) Å, and the Pt–Cl distances in **6** are 2.311 Å and 2.357(1) Å. Changing from chloride to carbide, the relative elongations of the *trans* bonds are 0.168 Å (7.8%) for **1**, 0.156 Å (7.3%) for **2**, 0.0198 Å (0.9%) for **5**, and 0.046 Å (2.0%) for **6**. This demonstrates that the
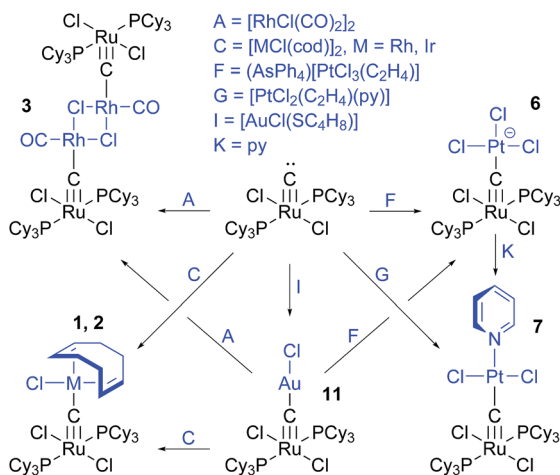
Scheme 2 Interconversions of carbide-bridged complexes.

structural *trans* influence of **RuC** is larger than that of Cl^- in complexes of Rh(I), Ir(I), Pd(II), and Pt(II).

2.4 Structural credence to π-backbonding

The formation of complexes **1–12** demonstrates that **RuC** coordinates well to electron-rich 2nd and 3rd row transition metals. Thus, the preferred reactivity of **RuC** resembles that of π-accepting ligands. Structurally, this type of ligands is characterized by forming short ligand–metal bonds in complexes with electron-rich metals. Along these lines, the identification of $\{Os(N)\}^{3+}$ and $\{Cr(N)\}^{2+}$ as back-bonding ligands towards electron-rich metal centres was partially based on structural evidence.[28,59]

The Cambridge Structural Database (CSD) allows a quantification of whether the metal-carbide bonds in **1–12** are short. Fig. 2 shows a histogram with all distances from carbon to Pd. For similar data for Rh, Ir, Pt, Ag, and Au, see ESI.† These diagrams and the percentile rank (Table 2) reveal that the metal-carbide bonds are at the very short end of the range of carbon–metal bonds (the shortest 0.5–17.6%) for all of these metals and characteristically similar to the respective metal-carbonyl bond lengths. This supports the notion that the ruthenium carbide acts as a π-accepting ligand.

A convincing juxtaposition of carbide complexes as ligands and CO as ligand requires kindred complexes of both ligand types. The existence of carbonyl analogues to **3, 4, 5, 6, 11**, and **12** provides for such a comparison, and suggests that the **RuC** and CO moieties play the same role in the respective complexes. The availability of X-ray crystal structures of $[RhCl(CO)_2]_2$,[60] $[IrCl(CO)_3]$,[61] $(Bu_4N)[PdCl_3(CO)]$,[62] (Bu = butyl) $(Bu_4N)[PtCl_3(CO)]$,[63] and $[AuCl(CO)]$[64] allows a direct comparison of the geometries of the carbonyl complexes and the structures of **1–12** (Table 3), and here it is relevant to note that **3** and **4** further allow a comparison of the **RuC** and CO ligands within the same complex. Though $Au(CO)_2^+$ is well established,[65–68] its crystal structure has not been reported.

In **3** and $[RhCl(CO)_2]_2$, the Rh–C bonds are 0.6–1.6% shorter for CO than for **RuC**. The Rh–Cl bonds *trans* to CO are equal within three standard deviations, whereas the bond *trans* to **RuC** is longer by 0.8%, suggesting a larger structural *trans* influence of **RuC** than of CO. The RuC–Ir bonds in **4** fall within the range found for *trans* carbonyls in $[IrCl(CO)_3]$. Contrarily,
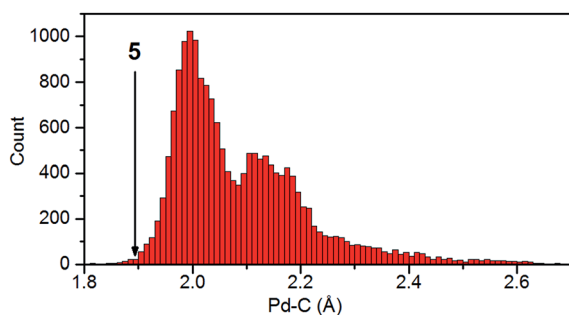

Fig. 2 Pd–C distances from the CSD (v.1.16); the arrow indicates the position of the carbide–palladium bond in **5**.

Table 3 Metrics for **3, 4, 5, 6, 11**, and analogous carbonyl complexes (Å and °)

3		$[RhCl(CO)_2]_2$	
Rh–C^a	1.864(3)	Rh–C	1.853(9)
Rh–C^b	1.835(2)	Rh–C	1.840(8)
Rh–Cl^c	2.403(1)	Rh–Cl	2.386(2)
Rh–Cl^d	2.384(1)	Rh–Cl	2.382(2)
4		$[IrCl(CO)_3]$	
Ir–C^a	1.988(5)	Ir–C^d	2.04(5)
Ir–C^a	1.974(5)	Ir–C^d	1.974(8)
Ir–C^b	1.785(11)	Ir–C^e	1.915(7), 1.903(9)
Ir–Cl	2.416(4)	Ir–Cl	2.317(10), 2.369(2)
Ir–C^a	1.988(5)	Ir–C^d	2.04(5)
Ir–C^a	1.974(5)	Ir–C^d	1.974(8)
5		$(Bu_4N)[PdCl_3(CO)]$	
Pd–C	1.892(2)	Pd–C	1.87(1)
Pd–Cl^c	2.3276(7)	Pd–Cl^d	2.283(2)
Pd–Cl^e	2.3076(7)	Pd–Cl^e	2.289(4)
Pd–Cl^e	2.3081(7)	Pd–Cl^e	2.295(3)
6		$(Bu_4N)[PtCl_3(CO)]$	
Pt–C	1.873(3)	Pt–C	1.825(6)
Pt–Cl^c	2.357(1)	Pt–Cl^d	2.289(7)
Pt–Cl^e	2.309(1)	Pt–Cl^e	2.289(2)
Pt–Cl^e	2.313(1)	Pt–Cl^e	2.295(2)
11		$[AuCl(CO)]$	
Au–C	1.921(3)	Au–C	1.93(2)
Au–Cl	2.2630(10)	Au–Cl	2.261(6)
C–Au–Cl	177.27(10)	C–Au–Cl	180

^{a} Carbide C. ^{b} Carbonyl C. ^{c} *trans* to C^{4-}. ^{d} *trans* to CO. ^{e} *trans* to Cl.

carbonyls *trans* to Cl form comparably short bonds in **4** and $[IrCl(CO)_3]$, particularly within **4**, where the Ir–C bond lengths are much shorter for CO than for **RuC** (on average shorter by 0.196 Å). This can in part be ascribed to electronic effects, but also the steric bulk of the **RuC** units (*vide supra*) may contribute to the elongation of the RuC–Ir bonds in the trinuclear complex.

The Pd–CRu bond in **5** is likely longer than the Pd–CO bond in $(Bu_4N)[PdCl_3(CO)]$, but the experimental uncertainty on the bond length in the carbonyl complex is too large to allow safe conclusions. In **5**, the Pd–Cl bond *trans* to the carbide is elongated (0.0198 Å, 0.9%) compared to the Pd–Cl bonds *trans* to Cl^-. Contrarily, all Pd–Cl bonds in $(Bu_4N)[PdCl_3(CO)]$ are similar in length, again demonstrating a larger structural *trans* influence of **RuC** than of CO. **6** and $(Bu_4N)[PtCl_3(CO)]$ show trends that parallel their Pd analogues with the Pt–CRu bond longer than the Pt–CO bond, but with **RuC** exhibiting a larger structural *trans* influence than chloride, whereas those of CO and chloride are comparable (see Table 3).

The strong similarity of **RuC** and CO as ligands is also borne out for coordination to Au(I) since $[AuCl(CO)]$ and **11** have nearly identical geometries around gold: the Au–C bonds are identical within 3σ between the two systems, and the same applies to the Au–Cl bonds. The gold(I) centres are linear in **11** (177.0(1)°) and $[AuCl(CO)]$ (180°).

Similarities between carbide and nitride complexes as ligands might be expected based on the isolobal relationship between M≡C: and M≡N: moieties. A direct comparison is made possible by the fact that **1**,[59,69–72] **2**,[71,73,74] **8**,[59,75] and **11** (ref. 40) have nitride-bridged analogues, [L_nMN–RhCl(cod)], [L_nMN–IrCl(cod)], [L_nMN–PtCl$_2$(dmso-S)], and [L_nMN–AuCl], where the ligand spheres only differ by **RuC** being replaced by a terminal nitride complex (Table 4). It has been argued that terminal nitride complexes act as strong π-accepting ligands[28] binding readily to electron-rich metal centres. The nitride bridges are linear like the carbide bridges in **1–12**. The rhodium and iridium nitride-bridged complexes display M–N bond lengths, which deviate significantly in both directions relative to the carbide-metal bond lengths in **1** and **2**. The longer bonds are present in complexes of Cr nitrides, Re nitrides, and [Os(N)O$_3$]$^-$; the relatively short bonds are present in complexes of Os(VI) nitrides, which, notably, are among the most electrophilic nitride complexes. Conversely, the N–Pt bonds in the CrN–Pt complexes are slightly shorter than or equal within 3σ to their carbide analogue, **8**. The N–Au bond in [(Me$_2$PhP)$_3$Cl$_2$ReN–AuCl] is equal to those in **12** within 3σ, though longer than that in **11**.

When **RuC** reacts with a stoichiometric amount of [Au(PPh$_3$)]OTf generated *in situ* from [AuCl(PPh$_3$)] and AgOTf, [(Cy$_3$P)$_2$Cl$_2$RuC–AuPPh$_3$]OTf initially forms. This species turns out to be unstable with respect to phosphine exchange, and subsequently, another **RuC** displaces PPh$_3$ from the Au(I) centre to yield **12**. The phosphine-containing intermediate has nitride-bridged analogues, namely [(Me$_3$SiCH$_2$)$_2$CpOsN–AuPPh$_3$]BF$_4$ (ref. 77) (Cp$^-$ = cyclopentadienide) and [O$_3$OsN–AuPPh$_3$].[38] The Au–N bonds are longer than the Au–C bonds in

12. Additionally, the homoleptic nitride-bridged Ag(I)-complex, [{(Me$_3$SiCH$_2$)$_2$CpOsN}$_2$Ag]BF$_4$,[76] resembles **12** with respect to connectivity. The nitride bridges are, however, distinctly bent compared to the carbide bridges in **12**, and the Ag–N bonds are longer than the Ag–C bonds in **9** and **10**.

Complexes of carbides and nitrides clearly show similar reactivities towards electron-rich metal centres, and yield structurally very similar bridged products. This suggests that the terminal carbide and nitride moieties interact similarly with electron-rich metal centres, *i.e.* with π-backdonation from the metal centres into low-lying π*-orbitals of the multiply-bonded carbides and nitrides.

3 Conclusions

We have demonstrated the ability of the ruthenium carbide, [Ru(C)Cl$_2$(PCy$_3$)$_2$] (**RuC**), to form linear carbide bridges to Rh(I), Ir(I), Pd(II), Pt(II), Ag(I), and Au(I). **RuC** binds readily to these low-valent metal centres, and the concomitant short bonds corroborate the view of the multiply bonded complex as a π-accepting ligand. The terminal carbide **RuC** forms similar complexes with closely matching geometries around the heterometals compared to the complexes formed by nitrides and carbon monoxide. The similarity in both structure and reactivity of **RuC** and strong π-accepting ligands yields further support to the π-acceptor nature of terminal carbides as ligands. The same conclusion derives from the large stretching frequency of CO in complex **4**, which suggests significant π-backdonation from Ir(I) to the **RuC** moiety. Generally, the structural *trans* influence of **RuC** is large and similar to or surpassing that of CO. The formations of **3** and **4** in stoichiometric reactions proceed through substitution of CO by **RuC**, showing that **RuC** binds to Rh(I) and Ir(I) with competitive strength to CO. These findings in conjunction with the large *trans* influence of **RuC** correspond well with the suggestion that terminal carbide complexes of group 8 metals are stronger σ-donating ligands than CO.[27] From the reactivity of **6** leading to substitution on Pt(II) in the position *trans* to the carbide ligand, a relatively high kinetic *trans* effect of the **RuC** moiety as a ligand can also be deduced.

In summary, earlier computationally based predictions, that M≡C: moieties should be able to outcompete CO as ligands and even form homoleptic metal complexes have been verified experimentally. Further studies extending this approach to molecular carbide complexes are ongoing.

Acknowledgements

Notes and references

Table 4 Nitride bridge metrics (°, Å) for M≡N–M′ complexes (M = Cr, Re, Os, M′ = Rh, Ir, Pt, Ag, Au)

Complex	M–N–M′	M–N	N–M′
[(dbm)$_2$CrN–RhCl(cod)]^{a,b,59}	171.8(1)	1.590(2)	1.971(2)
	170.5(1)	1.588(2)	1.970(2)
[(salen)CrN–RhCl(cod)]^{c,69}	173.04(9)	1.594(1)	1.959(1)
[(Me$_2$PhP)$_3$Cl$_2$ReN–RhCl(cod)]^{70}	174.8(4)	1.722(6)	1.956(6)
[(Ph$_3$As)$_2$Cl$_3$OsN–RhCl(cod)]^{71}	176.1(9)	1.675(9)	1.86(1)
[(Ph$_3$Sb)$_2$Cl$_3$OsN–RhCl(cod)]^{72}	175.3(4)	1.685(6)	1.847(6)
[(Me$_2$PhP)$_3$Cl$_2$ReN–IrCl(cod)]^{73}	173.9(6)	1.70(1)	1.96(1)
(Ph$_4$P)[O$_3$OsN–IrCl(cod)]^{73}	161.8(4)	1.693(7)	1.978(6)
[(Ph$_3$As)$_2$Cl$_3$OsN–IrCl(cod)]^{71}	176.2(9)	1.712(8)	1.816(8)
[(Ph$_3$Sb)$_2$Cl$_3$OsN–IrCl(cod)]^{74}	175.3(7)	1.71(1)	1.83(1)
[(dmso-O)(dbm)$_2$CrN–PtCl$_2$ (dmso-S)]^{b,59}	173.99(9)	1.618(1)	1.906(1)
[(acac)$_2$CrN–PtCl$_2$(dmso-S)]^{d,75}	172.3(1)	1.623(2)	1.901(2)
[{(Me$_3$SiCH$_2$)$_2$CpOsN}$_2$Ag]BF$_4$ (ref. 76)	166.7(9)	1.60(1)	2.15(1)
	162.6(9)	1.61(1)	2.12(1)
[(Me$_2$PhP)$_3$Cl$_2$ReN–AuCl]^{40}	173.8(1)	1.674(2)	1.969(2)
[(Me$_3$SiCH$_2$)$_2$CpOsN–AuPPh$_3$]BF$_4$ (ref. 77)	176.6(3)	1.675(4)	2.014(4)
[O$_3$OsN–AuPPh$_3$]^{38}	168(1)	1.69(2)	2.02(2)

^{a} Crystallizes with two crystallographically independent but connectively identical nitride bridges. ^{b} dbm$^-$ = dibenzoylmethanoate. ^{c} H$_2$salen = N,N'-bis(salicylidene)ethylenediamine. ^{d} acac$^-$ = acetylacetonate.

‡ Cod = 1,5-cyclooctadiene, PNP$^+$ = bis(triphenylphosphoranylidene)iminium, py = pyridine, dmso = dimethylsulfoxide, terpy = 2,2′:6′,2″-terpyridine, 4′-Ph-terpy = 4′-phenyl-2,2′:6′,2″-terpyridine.

1 T. Spatzal, M. Aksoyoglu, L. Zhang, S. L. A. Andrade, E. Schleicher, S. Weber, D. C. Rees and O. Einsle, *Science*, 2011, **334**, 940.

2 K. M. Lancaster, M. Roemelt, P. Ettenhuber, Y. Hu, M. W. Ribbe, F. Neese, U. Bergmann and S. DeBeer, *Science*, 2011, **334**, 974–977.

3 J. A. Wiig, Y. Hu, C. C. Lee and M. W. Ribbe, *Science*, 2012, **337**, 1672–1675.

4 J. A. Wiig, C. C. Lee, Y. Hu and M. W. Ribbe, *J. Am. Chem. Soc.*, 2013, **135**, 4982–4983.

5 F. Fischer and H. Tropsch, *Chem. Ber.*, 1926, **59**, 830–831.

6 F. Fischer and H. Tropsch, *Chem. Ber.*, 1926, **59**, 832–836.

7 C. K. Rofer-DePoorter, *Chem. Rev.*, 1981, **81**, 447–474.

8 R. L. Cordiner, A. F. Hill, R. Shang and A. C. Willis, *Organometallics*, 2010, **30**, 139–144.

9 M. Etienne, P. S. White and J. L. Templeton, *J. Am. Chem. Soc.*, 1991, **113**, 2324–2325.

10 A. F. Hill, M. Sharma and A. C. Willis, *Organometallics*, 2012, **31**, 2538–2542.

11 E. S. Borren, A. F. Hill, R. Shang, M. Sharma and A. C. Willis, *J. Am. Chem. Soc.*, 2013, **135**, 4942–4945.

12 A. L. Colebatch, R. L. Cordiner, A. F. Hill, K. T. H. D. Nguyen, R. Shang and A. C. Willis, *Organometallics*, 2009, **28**, 4394–4399.

13 J. C. Peters, A. L. Odom and C. C. Cummins, *Chem. Commun.*, 1997, 1995–1996, DOI: 10.1039/a704251e.

14 A. E. Enriquez, P. S. White and J. L. Templeton, *J. Am. Chem. Soc.*, 2001, **123**, 4992–5002.

15 R. G. Carlson, M. A. Gile, J. A. Heppert, M. H. Mason, D. R. Powell, D. V. Velde and J. M. Vilain, *J. Am. Chem. Soc.*, 2002, **124**, 1580–1581.

16 A. Hejl, T. M. Trnka, M. W. Day and R. H. Grubbs, *Chem. Commun.*, 2002, 2524–2525, DOI: 10.1039/B207903H.

17 S. R. Caskey, M. H. Stewart, J. E. Kivela, J. R. Sootsman, M. J. A. Johnson and J. W. Kampf, *J. Am. Chem. Soc.*, 2005, **127**, 16750–16751.

18 M. H. Stewart, M. J. A. Johnson and J. W. Kampf, *Organometallics*, 2007, **26**, 5102–5110.

19 P. E. Romero, W. E. Piers and R. McDonald, *Angew. Chem., Int. Ed.*, 2004, **43**, 6161–6165.

20 R. L. Miller, P. T. Wolczanski and A. L. Rheingold, *J. Am. Chem. Soc.*, 1993, **115**, 10422–10423.

21 S. R. Caskey, M. H. Stewart, M. J. A. Johnson and J. W. Kampf, *Angew. Chem., Int. Ed.*, 2006, **45**, 7422–7424.

22 Y. Mutoh, N. Kozono, M. Araki, N. Tsuchida, K. Takano and Y. Ishii, *Organometallics*, 2010, **29**, 519–522.

23 M. L. Macnaughtan, M. J. A. Johnson and J. W. Kampf, *J. Am. Chem. Soc.*, 2007, **129**, 7708–7709.

24 Y. Chen, W. Petz and G. Frenking, *Organometallics*, 2000, **19**, 2698–2706.

25 J. B. Gary, C. Buda, M. J. A. Johnson and B. D. Dunietz, *Organometallics*, 2008, **27**, 814–826.

26 A. Krapp, K. K. Pandey and G. Frenking, *J. Am. Chem. Soc.*, 2007, **129**, 7596–7610.

27 A. Krapp and G. Frenking, *J. Am. Chem. Soc.*, 2008, **130**, 16646–16658.

28 T. J. Crevier, S. Lovell and J. M. Mayer, *Chem. Commun.*, 1998, 2371–2372, DOI: 10.1039/a805277h.

29 R. G. Wilkins, in *Kinetics and Mechanism of Reactions of Transition Metal Complexes*, Wiley-VCH Verlag GmbH & Co. KGaA, 1991, p. 236, DOI: 10.1002/3527600825.ch4.

30 U. Belluco, L. Cattalini, F. Basolo, R. G. Pearson and A. Turco, *J. Am. Chem. Soc.*, 1965, **87**, 241–246.

31 L. Vaska and J. W. DiLuzio, *J. Am. Chem. Soc.*, 1961, **83**, 2784–2785.

32 R. Brady, W. H. De Camp, B. R. Flynn, M. L. Schneider, J. D. Scott, L. Vaska and M. F. Werneke, *Inorg. Chem.*, 1975, **14**, 2669–2675.

33 M.-A. Guillevic, A. M. Arif, J. A. Gladysz and I. T. Horváth, *Angew. Chem., Int. Ed. Engl.*, 1997, **36**, 1612–1615.

34 L. Vaska and L. S. Chen, *J. Chem. Soc. D*, 1971, 1080–1081, DOI: 10.1039/c29710001080.

35 M. Selke, W. L. Karney, S. I. Khan and C. S. Foote, *Inorg. Chem.*, 1995, **34**, 5715–5720.

36 F. Abu-Hasanayn, A. S. Goldman and K. Krogh-Jespersen, *Inorg. Chem.*, 1994, **33**, 5122–5130.

37 G. Pacchioni and P. S. Bagus, *Inorg. Chem.*, 1992, **31**, 4391–4398.

38 W.-H. Leung, J. L. C. Chim and W.-T. Wong, *J. Chem. Soc., Dalton Trans.*, 1996, 3153–3154, DOI: 10.1039/dt9960003153.

39 J. Chatt, C. D. Falk, G. J. Leigh and R. J. Paske, *J. Chem. Soc. A*, 1969, 2288–2293, DOI: 10.1039/J19690002288.

40 G. Beuter, U. Englert and J. Strähle, *Z. Naturforsch., B: J. Chem. Sci.*, 1988, **43**, 145–148.

41 R. Dantona, E. Schweda and J. Strähle, *Z. Naturforsch., B: Anorg. Chem., Org. Chem.*, 1984, **39**, 733–735.

42 C. Bach, H. Willner, F. Aubke, C. Wang, S. J. Rettig and J. Trotter, *Angew. Chem., Int. Ed. Engl.*, 1996, **35**, 1974–1976.

43 R. A. Wheeler, M. H. Whangbo, T. Hughbanks, R. Hoffmann, J. K. Burdett and T. A. Albright, *J. Am. Chem. Soc.*, 1986, **108**, 2222–2236.

44 A. Caselli, E. Solari, R. Scopelliti and C. Floriani, *J. Am. Chem. Soc.*, 2000, **122**, 538–539.

45 R. D. Young, A. F. Hill, G. E. Cavigliasso and R. Stranger, *Angew. Chem., Int. Ed.*, 2013, **52**, 3699–3702.

46 D. Mansuy, J. P. Lecomte, J. C. Chottard and J. F. Bartoli, *Inorg. Chem.*, 1981, **20**, 3119–3121.

47 V. L. Goedken, M. R. Deakin and L. A. Bottomley, *J. Chem. Soc., Chem. Commun.*, 1982, 607–608, DOI: 10.1039/c39820000607.

48 L. Galich, A. Kienast, H. Hückstädt and H. Homborg, *Z. Anorg. Allg. Chem.*, 1998, **624**, 1235–1242.

49 G. Rossi, V. L. Goedken and C. Ercolani, *J. Chem. Soc., Chem. Commun.*, 1988, 46–47, DOI: 10.1039/c39880000046.

50 A. Kienast, L. Galich, K. S. Murray, B. Moubaraki, G. Lazarev, J. D. Cashion and H. Homborg, *J. Porphyrins Phthalocyanines*, 1997, **1**, 141–157.

51 E. Solari, S. Antonijevic, S. Gauthier, R. Scopelliti and K. Severin, *Eur. J. Inorg. Chem.*, 2007, **2007**, 367–371.

52 F. Scherbaum, A. Grohmann, B. Huber, C. Krüger and H. Schmidbaur, *Angew. Chem., Int. Ed. Engl.*, 1988, **27**, 1544–1546.
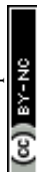
53 F. Scherbaum, A. Grohmann, G. Müller and H. Schmidbaur, *Angew. Chem., Int. Ed. Engl.*, 1989, **28**, 463–465.

54 O. Steigelmann, P. Bissinger and H. Schmidbaur, *Angew. Chem., Int. Ed. Engl.*, 1990, **29**, 1399–1400.

55 H. Schmidbaur, B. Brachthäuser, O. Steigelmann and H. Beruda, *Chem. Ber.*, 1992, **125**, 2705–2710.

56 F. P. Gabbaï, A. Schier, J. Riede and H. Schmidbaur, *Chem. Ber.*, 1997, **130**, 111–114.

57 J.-H. Jia and Q.-M. Wang, *J. Am. Chem. Soc.*, 2009, **131**, 16634–16635.

58 J.-H. Jia, J.-X. Liang, Z. Lei, Z.-X. Cao and Q.-M. Wang, *Chem. Commun.*, 2011, **47**, 4739–4741.

59 J. Bendix, C. Anthon, M. Schau-Magnussen, T. Brock-Nannestad, J. Vibenholt, M. Rehman and S. P. A. Sauer, *Angew. Chem., Int. Ed.*, 2011, **50**, 4480–4483.

60 L. Walz and P. Scheer, *Acta Crystallogr., Sect. C: Cryst. Struct. Commun.*, 1991, **47**, 640–641.

61 A. H. Reis, V. S. Hagley and S. W. Peterson, *J. Am. Chem. Soc.*, 1977, **99**, 4184–4186.

62 B. P. Andreini, D. Belli Dell'Amico, F. Calderazzo, M. G. Venturi and G. Pelizzi, *J. Organomet. Chem.*, 1988, **354**, 369–380.

63 D. R. Russell, P. A. Tucker and S. Wilson, *J. Organomet. Chem.*, 1976, **104**, 387–392.

64 P. G. Jones, *Z. Naturforsch., B: Anorg. Chem., Org. Chem.*, 1982, 823–824.

65 H. Willner and F. Aubke, *Inorg. Chem.*, 1990, **29**, 2195–2200.

66 M. Adelhelm, W. Bacher, E. G. Höhn and E. Jacob, *Chem. Ber.*, 1991, **124**, 1559–1561.

67 Q. Xu, Y. Imamura, M. Fujiwara and Y. Souma, *J. Org. Chem.*, 1997, **62**, 1594–1598.

68 H. Willner, J. Schaebs, G. Hwang, F. Mistry, R. Jones, J. Trotter and F. Aubke, *J. Am. Chem. Soc.*, 1992, **114**, 8972–8980.

69 J. Vibenholt, M. Magnussen, C. Anthon and J. Bendix, *Acta Crystallogr., Sect. C: Cryst. Struct. Commun.*, 2010, **66**, m177–m179.

70 S. Schwarz and J. Strähle, *Z. Anorg. Allg. Chem.*, 2003, **629**, 493–496.

71 D. Morrogh, M. Galceran Mestres, E. Niquet, C. F. Barboza da Silva, A. Santos Saez, S. Schwarz and J. Strähle, *Z. Anorg. Allg. Chem.*, 2005, **631**, 1113–1118.

72 S. Schwarz, M. Galceran Mestres, E. Niquet, C. F. Barboza da Silva and J. Strähle, *Z. Naturforsch., B: J. Chem. Sci.*, 2004, **59**, 167–173.

73 S. Schwarz, E. Niquet, A. Santos Saez, M. Cots Pascual and J. Strähle, *Z. Anorg. Allg. Chem.*, 2003, **629**, 2479–2484.

74 D. Morrogh, S. Schwarz, C. Maichle-Mössmer and J. Strähle, *Z. Anorg. Allg. Chem.*, 2006, **632**, 801–806.

75 E. D. Hedegaard, M. Schau-Magnussen and J. Bendix, *Inorg. Chem. Commun.*, 2011, **14**, 719–721.

76 R. W. Marshman, J. M. Shusta, S. R. Wilson and P. A. Shapley, *Organometallics*, 1991, **10**, 1671–1676.

77 C. M. Lutz, S. R. Wilson and P. A. Shapley, *Organometallics*, 2005, **24**, 3350–3353.